ISBN: 978-3-95450-223-3 ISSN: 2673-7000 doi:10.18429/JACoW-NAPAC2019-TUYBA4

OPTIMIZATION OF AN SRF GUN DESIGN FOR UEM APPLICATIONS*

A. Liu†, R. Kostin, Euclid Techlabs, LLC, Bolingbrook, IL, U.S.A.
C. Jing, P. Avrakhov, Euclid Beamlabs, LLC, Bolingbrook, IL, U.S.A.

Abstract

Benefiting from the rapid progress on RF photogun technologies in the past two decades, the development of MeV-range ultrafast electron diffraction/microscopy (UED and UEM) has been identified as an enabling instrumentation. UEM or UED use low power electron beams with modest energies of a few MeV to study ultrafast phenomena in a variety of novel and exotic materials. SRF photoguns become a promising candidate to produce highly stable electrons for UEM/UED applications because of the ultrahigh shot-to-shot stability compared to room temperature RF photoguns. Euclid is developing a continuous wave (CW), 1.5-cell, MeV-scale SRF photogun operating at 1.3 GHz. In order to achieve the optimal beam parameters for the UED/UEM applications, the shape of the back wall is optimized by a heuristic Genetic Algorithm (GA) provided by a Python optimization package pyaopt. In this paper, the technical details of the design and preliminary optimization results are presented.

INTRODUCTION

The Basic Energy Science (BES) Workshop on the Future of Electron Scattering and Diffraction, held in 2014, identifies the objectives of pushing the boundaries of existing UED and UEM instruments, for which the desired electron beam parameters are given in Table 1. Specifically, the aggressive pursuit of sampling rates in the GHz range with extreme space-time resolution (STR) of 1 nm/10 nm and 100 fs/10 ps was strongly recommended. In an UED/UEM, stable femtosecond (fs) electron bunches, synchronized with laser pulses that excite transitions in the materials are needed. UEM/UED also has a stringent requirement on the shot-to-shot stability of beam energy and timing, which is difficult for a room temperature RF photogun to guarantee (typical jitter is on the order of 100 fs) [1].

Table 1: Desired Beam Parameters for Future UED/UEM

	UED	UEM
Charge	10 fC - 0.5 pC	0.5-1 pC
Bunch length	10 fs	ns - ps
Energy spread	10^{-4}	10^{-5}
Repetition rate	up to MHz	up to 100 Hz

The photogun in an UEM needs to minimize the energy spread (dE/E) and emittance (ϵ) to eliminate chromatic effects in the strong magnetic lenses, where a large dE/E introduces a spread in focal length. Ultimately a single-shot UEM requires the electron pulse to have $\epsilon_n \sim 10$ nm and $dE/E < 10^{-5}$. The state-of-the-art high-gradient S-band RF photoinjector can offer ∼ 0.1 pC, ∼ 10 nm emittance and ∼ 10^{-4} dE/E, however the MW-level pulsed RF source driving the photogun limits its application. This can be easily solved by using an SRF photogun. It operates at an ultrahigh Q in a CW mode, but only dissipates a few watts of RF power.

The R&D of SRF guns has made significant progress since first proposed [2, 3]. Tens of MV/m axial electric field has been achieved at the superconducting cathode. One of the biggest "showstoppers" for using an SRF photogun is that it introduces high fabrication and operation costs. On the one hand, to date, the application of SRF technologies to UEM has mainly focused on the superconducting objective lens [4]. On the other hand, The UED group at SLAC recently successfully initiated the use of an SRF electron source to upgrade the facility performance [5].

Euclid is developing a CW, 1.5-cell SRF gun operating at 1.3 GHz for UED/UEM applications. The project is funded by the DoE SBIR Phase II program. The design is being optimized and finalized for fabrications. In the following sections, the concept of the design, technical approach and the recent optimization results from running a GA on the shape of the back wall are presented.

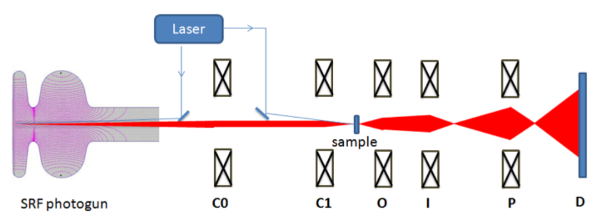

Figure 1: Schematic layout of the SRF photogun-based UEM system.

DESIGN CONCEPT

Figure 1 shows the schematic drawing of an SRF photogun-based UEM system. Besides the SRF cavity, it also includes a high repetition-rate laser system that generates both the pump and photoemission laser pulses, and magnetic lenses for the electron optics. A low-level RF (LLRF) control system manages the amplitude of the accelerating fields in the SRF cavity, which will operate in a phase-locked loop mode. It also synchronizes the laser with the SRF gun and monitors the arrival time of the e-beam at the beam dump/diagnostics. Benefiting from the CW operation, the RF amplitude and phase can be accurately

* Work supported by the SBIR program of the U.S. Department of Energy, under grant DE-SC0018621
† a.liu@euclidtechlabs.com

ISBN: 978-3-95450-223-3 ISSN: 2673-7000 doi:10.18429/JACoW-NAPAC2019-TUYBA4

controlled with precision below 100 ppm and 0.01 degree, respectively.

The back wall of the SRF cavity is used as a photocathode, which is illuminated by milliWatts of a UV laser. Since the required bunch charge is as small as 500 fC or even smaller, the quantum efficiency (QE) of Niobium (Nb) will be sufficient. A back wall photocathode design also is more robust than a plug-in type superconducting photocathode and avoids possible mechanical issues. Moreover, the metal photocathode is more robust against vacuum spikes and ion back-bombardment.

TECHNICAL DETAILS

Euclid has been working on a novel conduction cooling technology and coating technology together with Fermi National Accelerator Laboratory (FNAL). The technologies enable the use of Nb_3Sn instead of pure Nb, such that the entire system can run using a commercially available cryocooler free of liquid Helium, which sufficient to compensate the estimated 2 W heat load [6]. The application of conduction cooling and coating greatly reduces the operation complexity and costs. Moreover, the 2 W estimated RF power needed by the SRF photogun can be easily produced by a commercial product. Moreover, a fast SRF cavity tuner based on the patented Euclid ferroelectric technology can be used to compensate the phase or frequency change induced by effects like microphonics or Lorentz force.

The back wall of bare Nb (high RRR niobium, masked from the Sn coating) cavity as a photocathode. As was demonstrated in [7], the quantum efficiency of a bare Nb surface can exceed 10^{-5} at 266 nm. This is a robust photocathode configuration, and only requires mW-scale UV laser power.

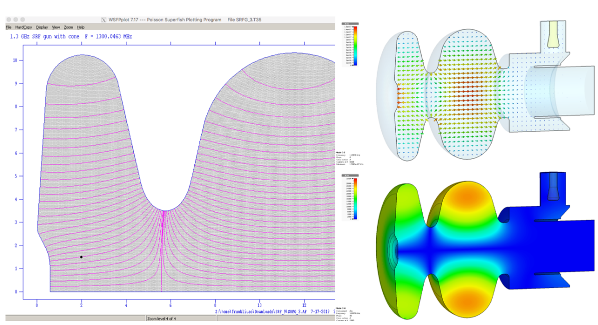

Figure 2: Autofish and CST simulation results of the first version with nose.

The cavity design process started with a manual tuning of the first 0.5-cell length. To be exact, the 0.X-cell is a more accurate description of the length of the first geometric structure. The manual tuning of the length compares the beam energy, maximum energy RF phase (at the emission), minimum energy spread phase. A brief summary is given in Table 2. In order to match the two optimal phases simultaneously, a novel "nose"-structure design was introduced in the first version. The nose not only helps to provide the optimal beam parameters, but also increases the mechanical strength, because of the inward-slope, as shown in Fig. 2. Its corresponding parameters are summarized in Table 3.

Table 2: Parameters of the 1.3 GHz SRF Photogun Cavity with Different 1.X-cell Lengths.

cell structure	1.5	1.45	1.4	1.35
Max. E [MeV]	1.7	1.6	1.5	1.4
Max. E phase [°]	20.5	23.2	28.3	33.3
Min. dE/E phase [°]	10.2	0	0	33.3

Table 3: Parameters of the 1.3 GHz Photogun Shown in Fig. 2.

Parameter	Value
Length	1.45 cell
Q_0 at 4° K ($R_s = 20\ n\Omega$)	1.16×10^{10}
R/Q (critical coupling)	176.9 Ω
Geometry factor	232 Ω
Wall power dissipation	0.9 W
E_{max}	23.5 MV/m
B_{max}	43.3 mT

Beam tracking results

Considering the QE of bare Nb surface at the back wall of the 1.5 cell photogun is approximately 10^{-5} at 266 nm, a high repetition rate, fC-level pulsed electron bunch emission can be achieved without an amplifier. With an amplifier, a kHz repetition rate with 500 fC per bunch can be achieved. In the simulations, various parameters are assumed for the emitted beam bunch as the initial beam for tracking. The tracking was with space charge effect included, and primarily done using Astra [8] then cross-checked using GPT [9].

Mainly two cases are considered in the Astra simulations. The first case features an ultra-low charge (5 fC) per bunch, with an ultrashort laser pulse of 15 fs full-width-half-maximum (FWHM) that has a diameter of 36 μm (a UED-compatible configuration). In the other case, a 500 fC bunch charge is assumed, with the laser spot size and laser pulse FWHM at 180 μm and 70 fs, respectively (a UEM-compatible configuration). The parameter evolution from the back wall photocathode emission to 1 meter downstream of the back wall is shown in Fig. 3. Notice that no solenoid was added in the simulations. Adding the solenoid is considered an option to further increase the performance of the SRF photogun.

HEURISTIC OPTIMIZATIONS

The back wall nose design was further optimized using a GA, built in the Python package `pyaopt` [10, 11]. The package includes multiple widely-accepted algorithms such as GA, Simulated Annealing (SA) and the Particle Swarm Algorithm (PSA), etc.

North American Particle Acc. Conf. NAPAC2019, Lansing, MI, USA JACoW Publishing
ISBN: 978-3-95450-223-3 ISSN: 2673-7000 doi:10.18429/JACoW-NAPAC2019-TUYBA4

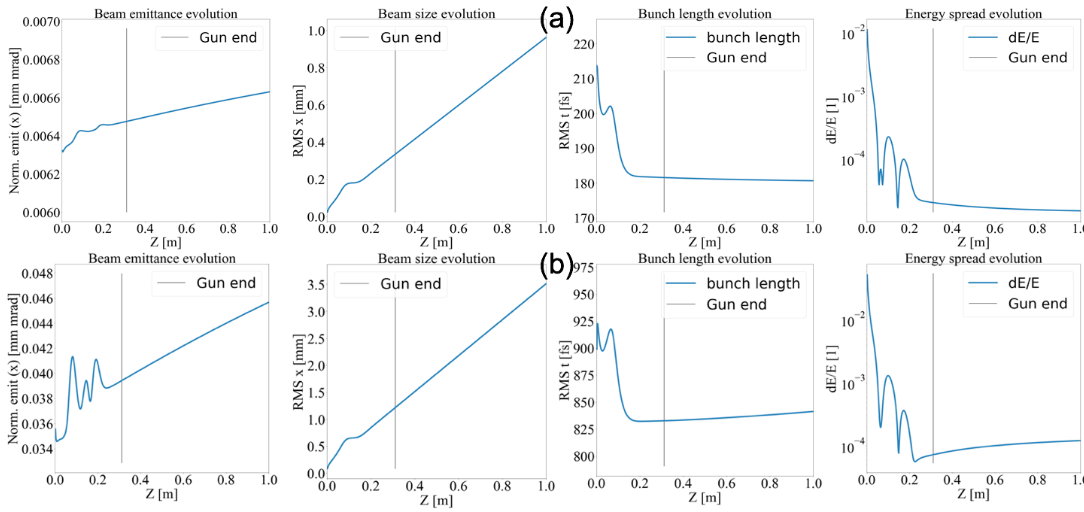

Figure 3: Important beam parameter evolution from the back wall photocathode to 1 meter downstream of the back wall. (a) corresponds to case 1, (b) is for case 2.

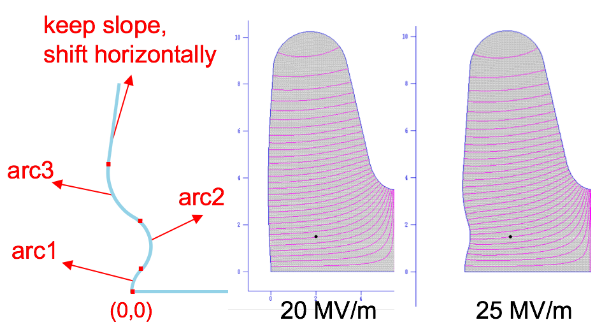

Figure 4: The nose shape used in the optimization and the GA-optimized shapes for 20 MV/m and 25 MV/m E_{acc}.

The optimization was done with a few nose shapes, which keep the inward slope but varies the arcs at the nose. There are two objectives set for the algorithm, which are to minimize the dE/E and minimize the bunch length 1 meter downstream of the back wall. A schematic drawing of the most promising design and the optimized shapes for scenarios with E_{acc} = 20 MV/m and 25 MV/m are shown in Fig. 4. The results indicate that the optimal shape for different maximum axial electric field achievable has noticeable differences. The UED bunch configuration was used as the initial beam in the optimization.

The algorithm was efficient in finding not only an optimum shape, but also a correct RF phase for the photoemission. This is exciting, considering the optimum phase for different shapes also differs. Because the original design discussed in the previous sections was a result of some initial scan optimizations, the first scenario (E_{acc} = 20 MV/m) only resulted in a small improvement from the original. This however also confirms the robustness of the original design, and also suggests that the performance may be limited by the fixed slope of the wall. At 5fC, 15 fs FWHM, 36 μm laser spot, the 1-meter downstream beam parameters are σ_t = 181 for both designs, and $dE/E = 1.52 \times 10^{-5}$ and 1.22×10^{-5} for the original and GA-optimized designs, respectively.

As for the E_{acc} = 25 MV/m scenario, the GA yielded a significantly better performance than the original design at 25 MV/m. This suggests that further optimizations that include an improved objective function may greatly improve the optimal performance at higher electric field. At 5 fC, 15 fs FWHM, 36 μm laser spot, the 1-meter downstream beam parameters are σ_t = 267 fs and 226 fs, $dE/E = 4.86 \times 10^{-4}$ and 8.47×10^{-6} for the original and optimized designs, respectively. At 500 fC, 70 fs FWHM, 180 μm laser spot, the parameters are σ_t = 1073 fs and 920 fs, $dE/E = 1.83 \times 10^{-3}$ and 1.49×10^{-4} for the original and optimized designs, respectively.

CONCLUSION AND FUTURE WORK

An SRF photogun has been designed at Euclid for MeV UED/UEM applications. The innovative approach of using conductive cooling and Nb_3Sn coating makes the device more affordable and less likely to fail considering the back wall is used as a photocathode. Heuristic algorithms have been applied to the optimization of the nose structure of the back wall. The results indicate that the original scanned and tuned design has a near-optimum performance, and also that the inward slope can be changed to further improve the performance. The optimization shows that the optimum nose structure heavily depends on the achievable axial electric field. The optimization setup will be modified to consider more objective functions in the future work, aiming to find an optimum balanced design.

ACKNOWLEDGEMENTS

The authors would like to thank our collaborators, Dr. Yimei Zhu and Dr. Erdong Wang, at BNL, for their discussions and support. We also thank Dr. Gwanghui Ha at AWA of ANL for cross-checking the Astra simulations using GPT.

ISBN: 978-3-95450-223-3 ISSN: 2673-7000 doi:10.18429/JACoW-NAPAC2019-TUYBA4

REFERENCES

[1] I.V. Isaev *et al.*, "RF photo-gun stability measurement at PITZ", in *Proc. IPAC'11*, San Sebastián, Spain, p. 442–444, 2011.

[2] H. Chaloupka *et al.*, "A proposed superconducting photoemission source of high brightness", *Nucl. Instr. Meth. A*, vol. 285, p. 327, 1989.

[3] J. Sekutowicz, "SRF gun development overview", in *Proc. SRF'15*, Whistler, Canada, Sep. 2015, paper THAA02, pp. 994 - 1000.

[4] D. Xiang, "FEIS2015 presentation", http://www.bt.pa.msu.edu/FEIS-2/talks/FEIS-2_Xiang.pdf

[5] Chunguang Jing, Euclid Beamlabs, private communication.

[6] R. Dhuley *et al.*, "Thermal link design for conduction cooling of SRF cavities using cryocoolers", IEEE Trans. Appl. Supercond., vol. 29, p. 0500205, 2019.

[7] Porter, Ryan, "Potential for very high accelerating gradients with Nb3Sn SRF cavities", presented at Advanced Accelerator Concepts, 2018, unpublished.

[8] Astra, A Space Charge Tracking Algorithm, http://www.desy.de/~mpyflo/.

[9] GPT, General Particle Tracer, http://www.pulsar.nl/gpt/.

[10] A. Liu, P. V. Avrakhov, C.-J. Jing, and R. A. Kostin, "pyaopt Optimization Suite and its Applications to an SRF Cavity Design for UEMs", in *Proc. ICAP'18*, Key West, Florida, USA, Oct. 2018, pp. 229–232. doi:10.18429/JACoW-ICAP2018-TUPAF19

[11] A. Liu, D. Neuffer, and A. Bross, "Design and simulation of the nuSTORM pion beamline", *Nucl. Inst. Meth. A*, vol. 801, pp. 44-50, 2015. doi:10.1016/j.nima.2015.08.020